Fe(Co)SiBPCCu nanocrystalline alloys with high B s above 1.83 T

Article *in* Journal of Magnetism and Magnetic Materials · May 2017

DOI: 10.1016/j.jmmm.2017.05.072

Tao Liu
Ningbo Institute of Materials Technology and…

Anding Wang
City University of Hong Kong

Chuntao Chang
Ningbo Institute of Materials Technology and…

Journal of Magnetism and Magnetic Materials 441 (2017) 174–179

Contents lists available at ScienceDirect

Journal of Magnetism and Magnetic Materials

journal homepage: www.elsevier.com/locate/jmmm

Research articles

Fe(Co)SiBPCCu nanocrystalline alloys with high B_s above 1.83 T

Tao Liu [a,b], Fengyu Kong [c], Lei Xie [a], Anding Wang [a,d,*], Chuntao Chang [a,*], Xinmin Wang [a], Chain-Tsuan Liu [d]

[a] Key Laboratory of Magnetic Materials and Devices, Ningbo Institute of Materials Technology and Engineering, Chinese Academy of Sciences, Ningbo, Zhejiang 315201, China
[b] University of Chinese Academy of Sciences, 19 A Yuquan Rd, Shijingshan District, Beijing 100049, China
[c] School of Materials and Chemical Engineering, Ningbo University of Technology, Ningbo 315016, China
[d] Center for Advanced Structural Materials, Department of Mechanical and Biomedical Engineering, College of Science and Engineering, City University of Hong Kong, Kowloon, Hong Kong, China

ARTICLE INFO

Article history:
Received 10 January 2017
Received in revised form 23 May 2017
Accepted 23 May 2017
Available online 25 May 2017

Keywords:
Nanocrystalline alloy
High B_s
Magnetic property
Microstructure
Magnetic domain

ABSTRACT

$Fe_{84.75-x}Co_xSi_2B_9P_3C_{0.5}Cu_{0.75}$ ($x = 0$, 2.5 and 10) nanocrystalline alloys with excellent magnetic properties were successfully developed. The fully amorphous alloy ribbons exhibit wide temperature interval of 145–156 °C between the two crystallization events. It is found that the excessive substitution of Co for Fe greatly deteriorates the magnetic properties due to the non-uniform microstructure with coarse grains. The alloys with $x = 0$ and 2.5 exhibit high saturation magnetization (above 1.83 T), low core loss and relatively low coercivity (below 5.4 A/m) after annealing. In addition, the $Fe_{84.75}Si_2B_9P_3C_{0.5}Cu_{0.75}$ nanocrystalline alloy also exhibits good frequency properties and temperature stability. The excellent magnetic properties were explained by the uniform microstructure with small grain size and the wide magnetic domains of the alloy. Low raw material cost, good manufacturability and excellent magnetic properties will make these nanocrystalline alloys prospective candidates for transformer and motor cores.

1. Introduction

Fe-based amorphous and nanocrystalline alloys have attracted great interests, because of their excellent soft-magnetic properties and extremely low core loss, together with the low energy consumption and high efficiency process. The application in electricity generation, transmission and transformation fields is an attractive route for the preservation of environment problems [1-3]. However, their relatively lower saturation magnetization (B_s) compared with Si-steels is against the miniature of electromagnetic devices, which has limited their wide applications [4,5]. Hence, improving the B_s has been extremely desired, for the long-term targets of stronger, lighter, and higher efficiency devices [3,5,6].

Based on this, enormous efforts have been devoted to improve the B_s and the following effective methods are found: 1) Increasing the Fe content. By applying this widely-used method, many attempts failed because of the Fe content limitation based on the demand of the amorphous forming ability (AFA). The successful cases like FeSiBCu [7] and FeSiBPCu [8] still meet the harsh requirement of the ribbon production and annealing process [9]. Hence, more investigations are desired. 2) Substitution of Co for Fe. As accepted that the B_s of α-FeCo phase (2.45 T) is higher than that of α-Fe (2.18 T) [10], partial substitution of Co for Fe can effectively improve the B_s. Consequently, a series of Co-enhanced alloys with relatively higher B_s were developed, such as FeCoSiBCuNb [11], FeCoNbB [12], FeCoSiBPCu [13] etc. While we should also note that the effects of Co substitution is reported to be complicated, in some cases, drastic deterioration in soft-magnetic properties and a substantial increase of the material cost [14].

In this study, we proposed a brief composition design method for nanocrystalline alloys, as illustrated in Fig. 1. Three kinds of indispensable elements: ferromagnetic elements (Fe, Co), metalloid elements (Si, B, P and C) and nucleation motivating elements (Cu etc.) were chosen. Based on the consideration of B_s, the metallic elements with large atom size like Nb etc. which will lead to decrease of B_s, were eliminated. Relatively high Fe content is obtained by detailed investigation of AFA and competing precipitation process of α-Fe grains. The metalloid elements are selected from the aspects of AFA, manufacturability and the stability of the amorphous phase [15]. The Cu, which plays key role as nucleation sites, have great effect on AFA and annealing process as reported. The content is usually to be adjusted to a low value from

* Corresponding authors at: No. 1219 Zhongguan West Road, Zhenhai District, Ningbo City, Zhejiang Province 315201, China.
E-mail addresses: anding@nimte.ac.cn (A. Wang), ctchang@nimte.ac.cn (C. Chang).

http://dx.doi.org/10.1016/j.jmmm.2017.05.072
0304-8853/

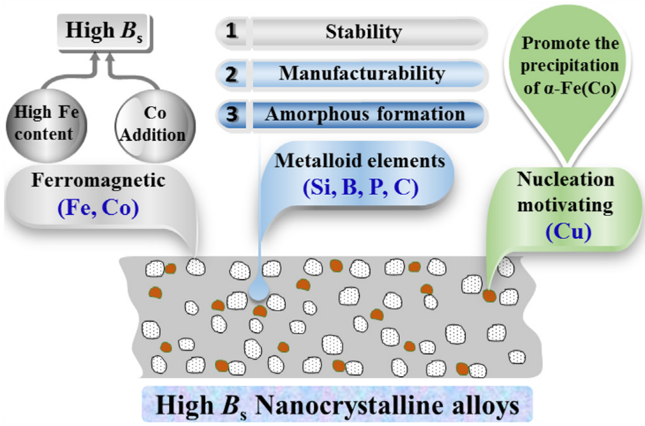

Fig. 1. The composition design of the $Fe_{84.75-x}Co_xSi_2B_9P_3C_{0.5}Cu_{0.75}$ high B_s nanocrystalline alloys.

the considering of wider ribbon production and annealing process windows [16,17]. The composition design method with considering synthetically from multiple factor for $Fe_{84.75}Si_2B_9P_3C_{0.5}Cu_{0.75}$ high B_s nanocrystalline alloys, together with the hysteresis losses and other alternating current properties will be reported later. Here, we focus on the excellent magnetic properties of these designed $Fe_{84.75-x}Co_xSi_2B_9P_3C_{0.5}Cu_{0.75}$ (x = 0, 2.5 and 10) nanocrystalline alloys. The magnetic properties of these alloys were characterized in detail. The microstructure and magnetic domains were also investigated. These results will give us a better insight of the nanocrystalline alloys and provide an effective composition design method of high B_s nanocrystalline alloys.

2. Material and methods

The master alloys of $Fe_{84.75-x}Co_xSi_2B_9P_3C_{0.5}Cu_{0.75}$ (x = 0, 2.5 and 10) were melt by induction melting under Ar atmosphere after high vacuum of about 1×10^{-2} Pa with pure elements of Fe (99.99 wt%), Co (99.9 wt%), Si (99.99 wt%), B (99.9 wt%), Cu (99.99 wt%) and pre-alloy of Fe_3P and Fe-3.6%C. Ribbons with width of about 1 mm and thickness of about 21 µm were prepared through single-roller melt-spinning method. The thermal properties were identified by differential scanning calorimetry (DSC, NETZSCH 404C) at a heating rate of 40 °C /min. Isothermal annealing was carried out under a certain temperature for 5 min followed by water-quenching. The microstructures of as-quenched and annealed ribbons were investigated by X-ray diffraction (XRD, Bruker D8 Advance) with Cu-Kα radiation and high-resolution transmission electron microscopy (TEM, TECNAI F20). The magnetic domain structure was observed on the air-bare surface by Magneto-optical Kerr Microscope without further sample preparation such as polishing or coating. The magnetic properties including saturation magnetization (B_s), coercivity (H_c), core loss (P) and effective permeability (μ_e) were measured with vibrating sample magnetometer (VSM, Lake Shore 7410) under the field of 800 kA/m, B-H loop tracer (EXPH-100) under the field of 800 A/m, AC B-H curve tracer (AC BH-100 K) and impedance analyzer (Agilent 4294 A) at different applied magnetic field (H_m), respectively. The changes of the magnetic force (generated by a magnet right above the samples) along with the temperature were measured by the thermogravimetric analyzer (Diamond TG/DTA).

3. Results and discussion

All ribbon samples prepared with the commonly used parameters exhibit good surface quality and ductility. The microstructures of these $Fe_{84.75-x}Co_xSi_2B_9P_3C_{0.5}Cu_{0.75}$ (x = 0, 2.5 and 10) alloy ribbons were identified by XRD from the free side. As depicted in Fig. 2, the only halo peak without any sharp crystalline peaks of the ribbons means the totally amorphous structure, which indicates the good AFA of these alloys. Here, we can conclude that the composition design method is reasonable and the substitution of Co for Fe in this alloy system does not decrease the AFA seriously.

Then, the thermal performance of the as-quenched $Fe_{84.75-x}Co_xSi_2B_9P_3C_{0.5}Cu_{0.75}$ (x = 0, 2.5 and 10) ribbons were investigated by DSC. Two distinct exothermic peaks, with the onset temperatures marking as T_{x1} and T_{x2}, can be easily observed in the curves as shown in Fig. 3. All these alloys exhibit a wide temperature interval ($\triangle T_x = T_{x2} - T_{x1}$) of 145–156 °C, which is much larger than the FePC(Si)Cu [18,19] and FeBC(Si)Cu [20] alloy systems and comparable to the typical FeSiBCu [7,21] and FeSiBPCu [8,22,23] alloy systems as shown in the inserted table. According to the previous study [24], the first and second crystallization peaks are corresponding to the precipitation of α-Fe phase and compounds like boride, phosphide etc., respectively. The large $\triangle T_x$ is favorable to control the precipitation of α-Fe in the amorphous matrix and form a uniform "α-Fe phase + residual amorphous" structure during the annealing process [8,25], which is beneficial for excellent magnetic properties. With the substitution of Co, T_{x1} shifts to the higher temperature slightly, which may be attributed to the decrease of the driving force for the Cu clustering in the Co-contained alloys [26]. While T_{x2} shifts to the higher temperature apparently, suggesting that the Co-contained alloys have higher stability of the residual amorphous phase.

It is known that the magnetic properties of nanocrystalline alloys is highly dependent on the annealing temperature (T_A). In order to determine the optimal annealing process, isothermal annealing under different temperature was carried out. The changes of H_c as a function of T_A for the $Fe_{84.75-x}Co_xSi_2B_9P_3C_{0.5}Cu_{0.75}$ (x = 0, 2.5 and 10) alloys were shown in Fig. 4. With the increase of T_A, the changes of H_c for the alloys with x = 0 and 2.5 behave a similar tendency that the H_c remains a small value (~5.0 A/m) in a wide temperature range. For the alloy with x = 10, the H_c is much larger (~16.0 A/m) even at the optimum annealing temperature range which is also much narrower compared to the alloy with x = 0 and 2.5. The difference of H_c between the $Fe_{84.75}Si_2B_9P_3C_{0.5}Cu_{0.75}$ and the 10 at% Co substituted alloys will be discussed later.

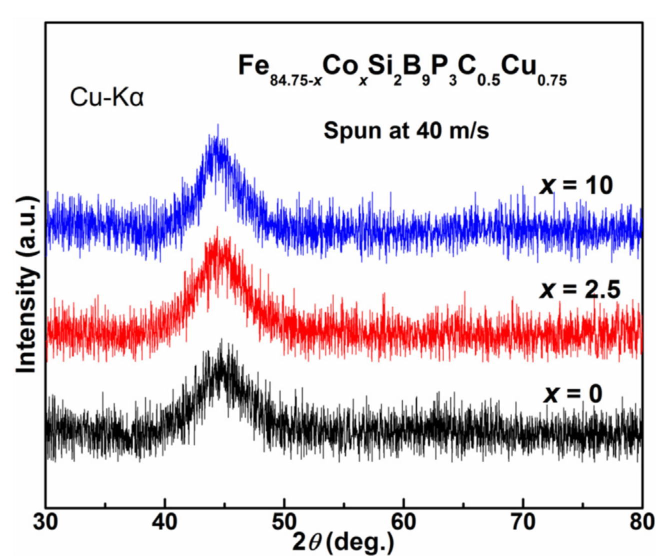

Fig. 2. XRD patterns of the as-quenched $Fe_{84.75-x}Co_xSi_2B_9P_3C_{0.5}Cu_{0.75}$ (x = 0, 2.5 and 10) ribbons.

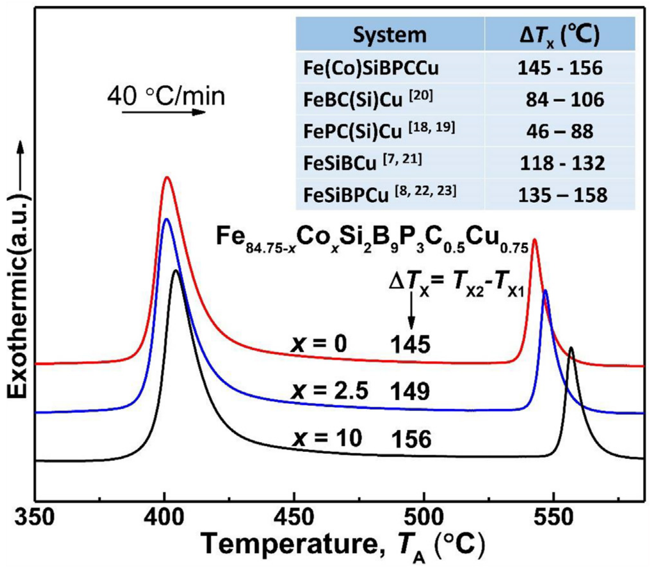

Fig. 3. DSC traces of the as-quenched $Fe_{84.75-x}Co_xSi_2B_9P_3C_{0.5}Cu_{0.75}$ ($x = 0$, 2.5 and 10) ribbons; Inserted table shows the $\triangle T_x$ of the typical nanocrystalline alloy systems.

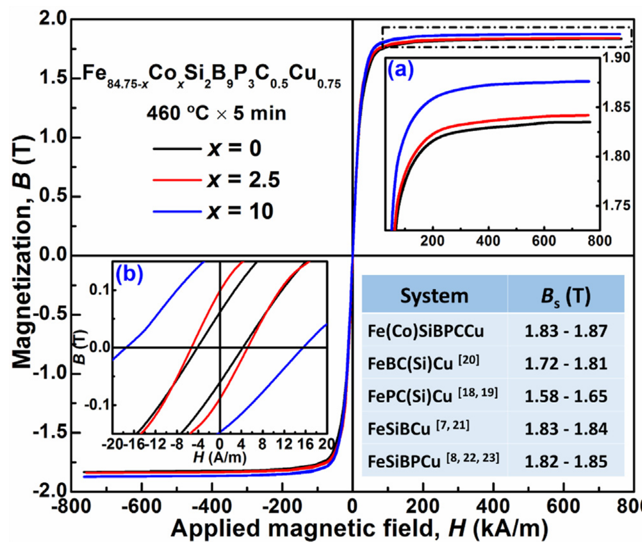

Fig. 5. Hysteresis loops of the $Fe_{84.75-x}Co_xSi_2B_9P_3C_{0.5}Cu_{0.75}$ ($x = 0$, 2.5 and 10) ribbons after annealing at optimum conditions; Inset (a) partially enlarged hysteresis loops; Inset (b) partially enlarged *B-H* loops; Inserted table shows the B_s for the typical nanocrystalline alloy systems.

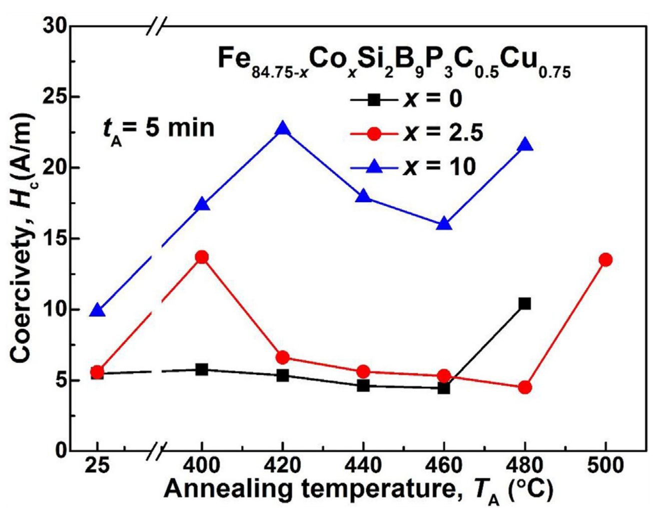

Fig. 4. H_c of the $Fe_{84.75-x}Co_xSi_2B_9P_3C_{0.5}Cu_{0.75}$ ($x = 0$, 2.5 and 10) ribbons dependence on T_A after annealing for 5 min.

According to the changes of H_c as a function of T_A, we determined the optimum annealing temperature is 460 °C. The hysteresis loops of these alloys after annealing at 460 °C for 5 min were shown in Fig. 5. With the substitution of Co for Fe, the B_s increases from 1.83 to 1.87 T as exhibited in the inset (a), while the H_c increases from 4.5 to 16.0 A/m as shown in the inset (b). These alloys exhibit attractively high B_s (above 1.83 T), which is much higher than the FePC(Si)Cu [18,19] and FeBC(Si)Cu [20] alloy systems after conventional annealing and comparable to the typical FeSiBCu [7,21] and FeSiBPCu [8,22,23] alloy systems after flash annealing, as shown in the inserted table.

As an important parameter for the magnetic materials, the core loss (P) of the designed alloys were then measured under different induction (B) and frequency (f). The changes of P as a function of B at 50 Hz for the $Fe_{84.75-x}Co_xSi_2B_9P_3C_{0.5}Cu_{0.75}$ ($x = 0$, 2.5 and 10) alloy ribbons were shown in Fig. 6(a), the P of the alloy with $x = 0$ is much lower than the Co-added alloys, especially for the alloy with $x = 10$, which is coincided with the changes of H_c in Fig. 5(a). Since the $Fe_{84.75}Si_2B_9P_3C_{0.5}Cu_{0.75}$ alloy exhibits much better soft-

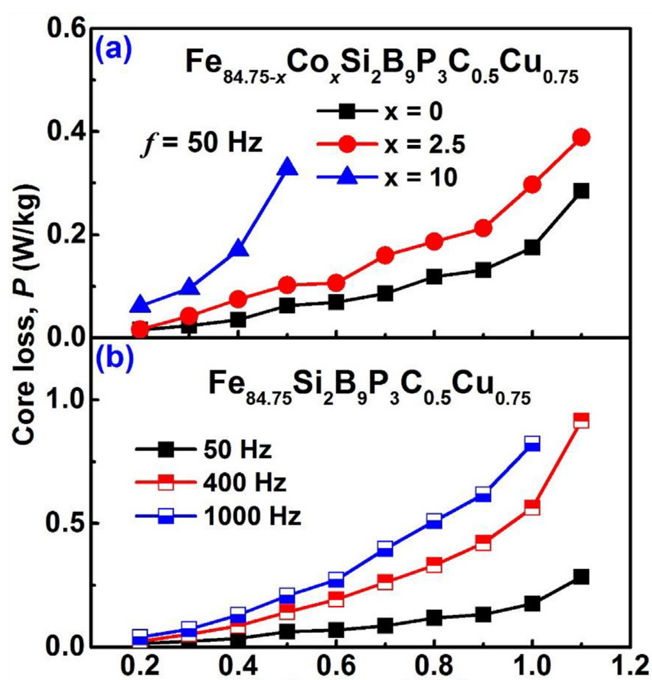

Fig. 6. Core loss of the ribbons after annealing at 460 °C for 5 min; (a) $Fe_{84.75-x}Co_xSi_2B_9P_3C_{0.5}Cu_{0.75}$ ($x = 0$, 2.5 and 10) alloy ribbons were measured at 50 Hz; (b) $Fe_{84.75}Si_2B_9P_3C_{0.5}Cu_{0.75}$ alloy ribbons were measured at 50 Hz, 400 Hz and 1000 Hz, respectively.

magnetic properties, the P of which under different f were further investigated. As shown in Fig. 6(b), the $Fe_{84.75}Si_2B_9P_3C_{0.5}Cu_{0.75}$ alloy exhibits a low $P_{50/1.0} = 0.17$ W/kg, $P_{400/1.0} = 0.56$ W/kg and $P_{1000/1.0} = 0.82$ W/kg, respectively, which is of great significance to be applied in motors and transformers etc.

Considering that the μ_e of the magnetic materials under different applied magnetic field (H_m) and frequency is an important parameter in terms of their applications [27,28], the μ_e on the dependence of the frequency for the $Fe_{84.75}Si_2B_9P_3C_{0.5}Cu_{0.75}$

nanocrystalline alloy was measured under different H_m. As shown in Fig. 7, with the increase of H_m, the μ_e increases from 1.2×10^4 ($H_m = 1$ A/m) to 2.8×10^4 ($H_m = 10$ A/m) and then decrease to 1.5×10^4 ($H_m = 20$ A/m) again at 400 Hz. It is interesting that the alloy exhibits excellent frequency properties at low H_m of 1 A/m and high H_m of 80–100 A/m, μ_e does not decrease distinctly in a wide range below cutoff frequency of about 20 kHz. The high μ_e above 1.2×10^4 and excellent frequency properties, will make the $Fe_{84.75}Si_2B_9P_3C_{0.5}Cu_{0.75}$ nanocrystalline alloy prospective candidates for various electric devices.

The magnetization (M_s) of the nanocrystalline alloys at the operating temperature should take into account as for their applications. Here, we use the TG/DTA to measure the magnetic force which is generated by a magnet right above the sample, then we convert the magnetic force to M_s by the formula as follows [29]:

$$F \times z = -\mu_0 V M_s \frac{\partial H}{\partial z}$$

Where F is the magnetic force, z is the distance between the sample and the magnet, V is the volume of the sample, $\frac{\partial H}{\partial z}$ is the magnetic field intensity induced by the magnet at a distance of z. Subsequently, the converted M_s is normalized according to the M_s measured by VSM at room temperature. Eventually, the measured M-T curves for the as-quenched and annealed $Fe_{84.75}Si_2B_9P_3C_{0.5}Cu_{0.75}$ ribbons were shown in Fig. 8. We can see that the M_s of the as-quenched ribbons decreases at the Curie temperature (about 293 °C) of the amorphous phase. The little drop in M_s and then increase slightly may be attributed to the clustering and crystallization take place at a relatively low temperature [30]. At about 410 °C, the crystallization of α-Fe result in a sharp increase of M_s. In comparison, we can easily observed that the annealed ribbons exhibit a much higher M_s without decline until 576 °C, this is due to the formation of α-Fe crystals with high Curie temperature. Since the M_s of a nanocrystalline alloy is the result of the coupling effect between residual amorphous phase and crystalline phase, the curie transition of the residual amorphous phase will not lead to the decrease of M_s [31]. In addition, the ferromagnetic-paramagnetic transition temperature of the nanocrystalline alloy ribbon is a little higher than the as-quenched ribbons, indicating a high crystallinity for the nanocrystalline alloys. Consequently, we can conclude that the $Fe_{84.75}Si_2B_9P_3C_{0.5}Cu_{0.75}$ nanocrystalline alloy exhibits a good temperature stability. These results also attest the importance of preparing nanocrystalline alloys from amorphous precursors, containing increase of B_s, decrease the λ_s [32] and improvement of the thermal stability of magnetic properties.

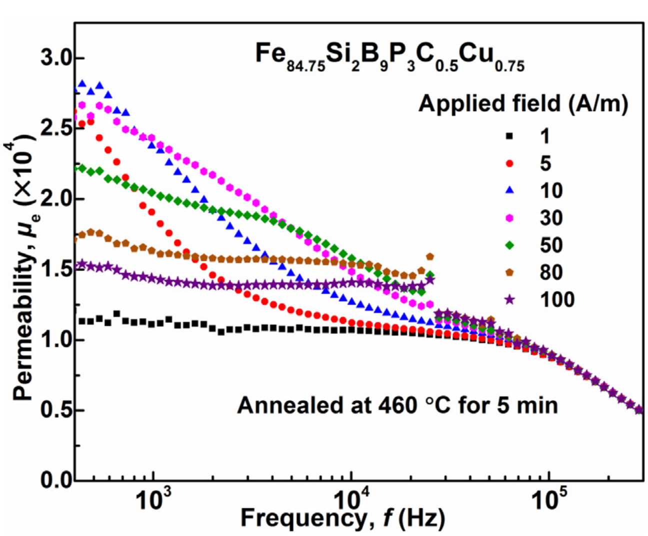

Fig. 7. The changes of μ_e as a function of frequency at different H_m from 400 Hz to 200 kHz for the $Fe_{84.75}Si_2B_9P_3C_{0.5}Cu_{0.75}$ nanocrystalline alloy.

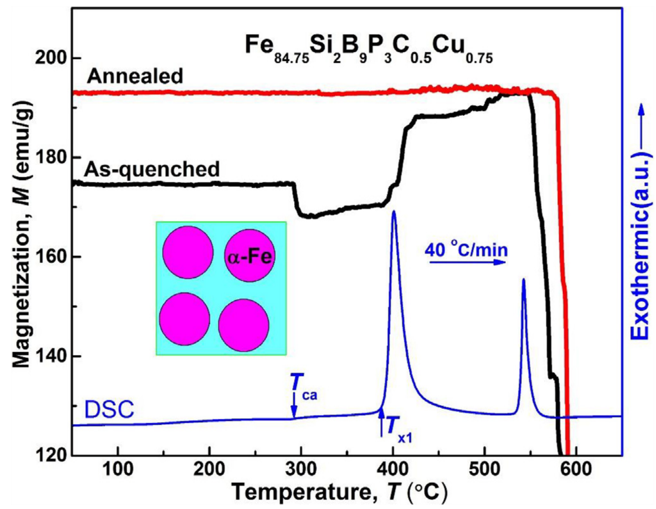

Fig. 8. Magnetization as a function of temperature for the $Fe_{84.75}Si_2B_9P_3C_{0.5}Cu_{0.75}$ ribbons after annealing under optimum conditions and as-quenched ribbons.

We explored the correlation among microstructure, magnetic domain structure and properties at last, for discussing the reason of excellent soft-magnetic properties of the $Fe_{84.75}Si_2B_9P_3C_{0.5}Cu_{0.75}$ alloy and the drastic H_c increase of the 10 at% Co substituted alloy. The TEM images selected area electron diffraction (SAED) patterns, grain size distribution and magnetic domains were shown in Fig. 9. In Fig. 9(a), we can observe that uniform microstructure with fine crystals and high crystallinity in the matrix is formed in the $Fe_{84.75}Si_2B_9P_3C_{0.5}Cu_{0.75}$ alloy. The crystals were identified as α-Fe from the SAED patterns in Fig. 9(b) and mean size of is about 22.8 nm as shown in Fig. 9(c). The uniform microstructure with small grain size is the reason for the excellent soft-magnetic properties [31]. In addition, smooth stripe domains separated by 180° walls along the sensitive direction, showing exiguous pinning centers, were clearly exhibited in Fig. 9(d). The large domain width which is inversely proportional to the domain wall energy [33], and correlated to the uniformity of microstructure [31] and anisotropy energy [12,31] also manifest the excellent soft-magnetic properties. In comparison, the distribution of the α-Fe(Co) is less uniform and the average grain size of the 10 at% Co substituted alloy is 31. 8 nm, which is much larger than the basic alloy, as shown in Fig. 9(e-g). It is speculated that the non-uniform microstructure with larger grain size of the Co-contained alloy is attributed to the decrease of the driving force for the Cu clustering as described in the DSC curves. This may result in a decrease of the nucleation sites, and then weak the competing effect of the grain growth, leading to a non-uniform microstructure with coarse grain size [31]. It has been reported that the magneto-crystalline anisotropy of α-Fe(Co) phase is higher than α-Fe [12,31], this may be the second reason for the increased H_c of Co-contained alloys.

4. Conclusions

High B_s $Fe_{84.75}Co_xSi_2B_9P_3C_{0.5}Cu_{0.75}$ (x = 0, 2.5 and 10) nanocrystalline alloys were successfully developed and the magnetic properties of these alloys were investigated in detail. The obtained results were summarized as follows:

1. The alloys were readily prepared into fully amorphous state with a large $\triangle T_x$ about 150 °C.

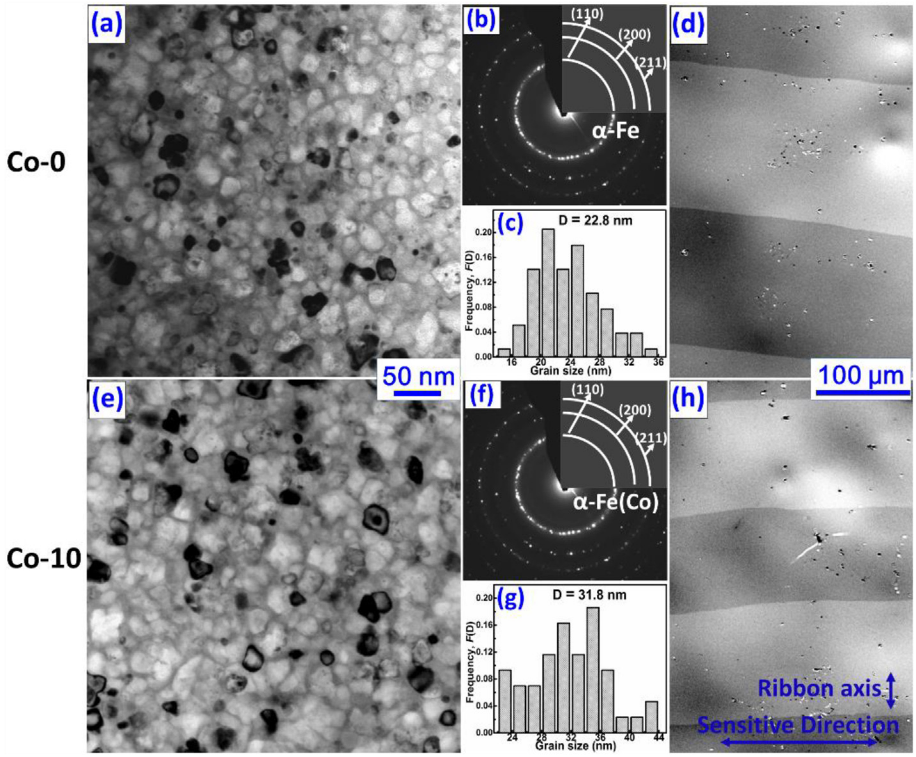

Fig. 9. TEM bright field images, SAED patterns and grain size distribution for the $Fe_{84.75-x}Co_xSi_2B_9P_3C_{0.5}Cu_{0.75}$ alloy (a–c) $x = 0$ and (e–g) $x = 10$; Magnetic domains of (d) $x = 0$ and (h) $x = 10$ ribbons after annealing under optimal temperature, respectively.

2. The alloys with $x = 0$ and 2.5 exhibit high B_s of 1.83–1.84 T, low H_c of 4.5–5.4 A/m after annealing under the optimal conditions. The B_s of the alloy with $x = 10$ increases to 1.87 T, but the H_c also drastically increases to 16.0 A/m.
3. The $Fe_{84.75}Si_2B_9P_3C_{0.5}Cu_{0.75}$ alloy shows low $P_{50/1.0} = 0.17$ W/kg, $P_{400/1.0} = 0.56$ W/kg and $P_{1000/1.0} = 0.82$ W/kg, respectively. Also exhibits high μ_e of 1.2–2.8 $\times$ 10^4 with excellent frequency properties and temperature stability.
4. The uniform microstructure with small grain size of 22.8 nm and a high crystallinity, and the wide magnetic domains with width of about 150 μm are the reasons for the excellent soft-magnetic properties of the $Fe_{84.75}Si_2B_9P_3C_{0.5}Cu_{0.75}$ alloy. For 10 at% Co substituted alloy, the microstructure is non-uniform with larger grain size of 31.8 nm and the domains is narrower.

Acknowledgement

This work was mainly supported by the National Natural Science Foundation of China (Grant No. 51601206, 51671206), Ningbo International Cooperation Projects (Grant No. 2015D10022) and Ningbo Major Project for Science and Technology (Grant No. 2014 01B1003003), Zhejiang Province Public Technology Research and Industrial Projects (Grant No. 2015C31043). AW and CTL were also supported by General Research Fund of Hong Kong under the grant number of CityU 102013.

References

[1] Y. Yoshizawa, Magnetic properties and applications of nanostructured soft magnetic materials, Scr. Mater. 44 (2001) 1321–1325.
[2] Y. Ogawa, M. Naoe, Y. Yoshizawa, R. Hasegawa, Magnetic properties of high Bs Fe-based amorphous material, J. Magn. Magn. Mater. 304 (2006) e675–e677.
[3] A. Wang, C. Zhao, H. Men, A. He, C. Chang, X. Wang, R.-W. Li, Fe-based amorphous alloys for wide ribbon production with high B-s and outstanding amorphous forming ability, J. Alloy. Compd. 630 (2015) 209–213.
[4] G. Herzer, Nanocrystalline soft magnetic alloys, Handbook of magnetic materials 10 (1997) 415–462.
[5] C. Zhao, A. Wang, A. He, S. Yue, C. Chang, X. Wang, R.-W. Li, Correlation between soft-magnetic properties and T-x1-T-c in high B-s FeCoSiBPC amorphous alloys, J. Alloy. Compd. 659 (2016) 193–197.
[6] D. Azuma, R. Hasegawa, Audible noise from amorphous metal and silicon steel-based transformer core, IEEE Trans. Magn. 44 (2008) 4104–4106.
[7] M. Ohta, Y. Yoshizawa, Magnetic properties of nanocrystalline Fe[sub 82.65]Cu [sub 1.35]Si[sub x]B[sub 16−x] alloys (x=0–7), Appl. Phys. Lett. 91 (2007) 062517.
[8] A. Makino, H. Men, T. Kubota, et al., New Fe-metalloids based nanocrystalline alloys with high Bs of 1.9 T and excellent magnetic softness, J. Appl. Phys. 105 (7) (2009) 07A308.
[9] M. Ohta Y. Yoshizawa Effect of heating rate on soft magnetic properties in nanocrystalline Fe80.5Cu1.5Si4B14 and Fe82Cu1Nb1Si4B12 alloys Appl. Phys. Exp. 2 2009 23005
[10] H. Ohno, Properties of ferromagnetic III–V semiconductors, J. Magn. Magn. Mater. 200 (1999) 110–129.
[11] C. Gómez-Polo, P. Marin, L. Pascual, et al. Structural and magnetic properties of nanocrystalline Fe73.5−xCoxSi13.5 B9CuNb3 alloys. Phys. Rev. B 2001 65(2) 024433.
[12] J.J. Ipus, J.S. Blázquez, V. Franco, A. Conde, Influence of Co addition on the magnetic properties and magnetocaloric effect of Nanoperm (Fe1−XCoX) 75Nb10B15 type alloys prepared by mechanical alloying, J. Alloy. Compd. 496 (2010) 7–12.
[13] R. Xiang, S.X. Zhou, B.S. Zong, G.Q. Zhang, Z.Z. Li, Y.G. Wang, C.T. Chang, Effect of Co addition on crystallization and magnetic properties of FeSiBPCu alloy, Prog. Nat. Sci.-Mater. Int. 24 (2014) 649–654.
[14] R.K. Roy, A.K. Panda, A. Mitra, Effect of Co content on structure and magnetic behaviors of high induction Fe-based amorphous alloys, J. Magn. Magn. Mater. 418 (2016) 236–241.
[15] K. Takenaka, A.D. Setyawan, P. Sharma, N. Nishiyama, A. Makino, Industrialization of nanocrystalline Fe–Si–B–P–Cu alloys for high magnetic flux density cores, J. Magn. Magn. Mater. 401 (2016) 479–483.
[16] M. Ohta, Y. Yoshizawa, Cu addition effect on soft magnetic properties in Fe–Si–B alloy system, J. Appl. Phys. 103 (7) (2008) 07E722.
[17] G.T. Xia, Y.G. Wang, J. Dai, Y.D. Dai, Effects of Cu cluster evolution on soft magnetic properties of Fe83B10C6Cu1 metallic glass in two-step annealing, J. Alloy. Compd. 690 (2017) 281–286.
[18] F.G. Chen, Y.G. Wang, Investigation of glass forming ability, thermal stability and soft magnetic properties of melt-spun Fe83P16-xSixCu1 (x=0, 1, 2, 3, 4, 5) alloy ribbons, J. Alloy. Compd. 584 (2014) 377–380.
[19] Y. Jin, X. Fan, H. Men, X. Liu, B. Shen, FePCCu nanocrystalline alloys with excellent soft magnetic properties, Sci. China Technol. Sci. 55 (2012) 3419–3424.

[20] X.D. Fan, H. Men, A.B. Ma, B.L. Shen, Soft magnetic properties in Fe84−xB10C6Cux nanocrystalline alloys, J. Magn. Magn. Mater. 326 (2013) 22–27.
[21] M. Ohta, Y. Yoshizawa, Magnetic properties of high Bs Fe–Cu–Si–B nanocrystalline soft magnetic alloys, J. Magn. Magn. Mater. 320 (20) (2008) e750–e753.
[22] A. Makino, H. Men, K. Yubuta, T. Kubota, Soft magnetic FeSiBPCu heteroamorphous alloys with high Fe content, J. Appl. Phys. 105 (2009) 013922.
[23] A. Makino, H. Men, T. Kubota, et al., New excellent soft magnetic FeSiBPCu nanocrystallized alloys with high Bs of 1.9 T from nanohetero-amorphous phase, IEEE Trans. Magn. 45 (10) (2009) 4302–4305.
[24] Z. Li, A. Wang, C. Chang, Y. Wang, B. Dong, S. Zhou, Synthesis of FeSiBPNbCu nanocrystalline soft-magnetic alloys with high saturation magnetization, J. Alloy. Compd. 611 (2014) 197–201.
[25] A. Inoue, Stabilization of metallic supercooled liquid and bulk amorphous alloys, Acta Mater. 48 (2000) 279–306.
[26] M. Ohnuma, D.H. Ping, T. Abe, H. Onodera, K. Hono, Y. Yoshizawa, Optimization of the microstructure and properties of Co-substituted Fe–Si–B–Nb–Cu nanocrystalline soft magnetic alloys, J. Appl. Phys. 93 (2003) 9186.
[27] J. Fuzerova, J. Fuzer, P. Kollar, R. Bures, M. Faberova, Complex permeability and core loss of soft magnetic Fe-based nanocrystalline powder cores, J. Magn. Magn. Mater. 345 (2013) 77–81.
[28] S. Dobák, J. Füzer, P. Kollár, Effect of a DC transverse magnetic field on the magnetization dynamics in FeCuNbSiB ribbons and derived nanostructured powder cores, J. Alloys Compd. 651 (2015) 237–244.
[29] D. Jiles, Introduction to magnetism and magnetic materials, CRC Press, 2015.
[30] P. Sharma, X. Zhang, Y. Zhang, A. Makino, Competition driven nanocrystallization in high Bs and low coreloss Fe–Si–B–P–Cu soft magnetic alloys, Scr. Mater. 95 (2015) 3–6.
[31] G. Herzer, Modern soft magnets: amorphous and nanocrystalline materials, Acta Mater. 61 (2013) 718–734.
[32] A. Makino, T. Kubota, K. Yubuta, et al., Low core losses and magnetic properties of Fe85-86Si1-2B8P4Cu1 nanocrystalline alloys with high B for power applications, J. Appl. Phys. 109 (7) (2011) 07A302.
[33] H. Kronmuller, M. Fahnle, M. Domann, H. Grimm, R. Grimm, B. Groger, Magnetic-properties of amorphous ferromagnetic-alloys, J. Magn. Magn. Mater. 13 (1979) 53–70.